AQUEOUS INTERFACES IN PLANT CELLS

S. K. Asunmaa[1]
Institute for Pure and Applied Physical Sciences,
University of California, San Diego, LaJolla, California 92037

ABSTRACT

A subunit, 90 to 100 Å in diameter, consisting of lipid and protein components, is proposed for semipermeable plant cell membranes. The hydrocarbon chains of the lipid molecules are oriented toward the periphery, the hydrophilic molecular segments toward the center of a lipid annulus where the hydrophilic region stabilizes a 22-Å sheath of ordered water, too rich in hydrogen bonds to dissolve electrolytes. The ordered water leaves a core of ordinary water for ion transport. The subunit thus acts as an ion-gate, because of synchronized movement of the lipids for opening and closing the pore, powered by surface adsorbed proteins. The subunit model would consist of 27 galactosyl diglyceride units (mono- or di- or both) in chloroplast membranes from which Wehrmeyer (1967) isolated a 80,000-g fraction that consists of 90-Å diameter subunits.

Membrane permeability data and the Small-Bourgès (1965) phase diagram for the ternary system cholesterol-lecithin-water (in agreement with X-ray and NMR data) are discussed as supporting evidence for the ion-gate model, after a short review of the model design for the cholesterol-lecithin complexes, which in the subunit configuration may adsorb proteins such as the circular polypeptide alamethicin. The role of plant proteins requires further analysis. Electron micrographs of preparations of plant cell membranes, animal cell plasma membranes and proteolipid membranes *in vitro*, as published by various research groups, are presented as morphological support for the ion-gate model.

INTRODUCTION

At the time when electron micrographs of the osmium-fixed living cell have depicted the various cell organelles and their mutual locations and the more gentle fixations have moved the interest to the dimensions and structures at the molecular level, it is tempting to design molecular models for *in vivo* material and try to correlate the various realms of information available. When electron micrographs are being extrapolated to *in vivo* conditions, the aqueous interfaces and the plasmasol physical properties including the liquid crystalline state of matter require a special discussion.

A model of an ion-gate in thin proteolipid membranes was recently designed, using a circular array of cholesterol-lecithin complexes, for the animal cell plasma membrane (Schultz, Asunmaa, and Kleist 1969; Asunmaa, Schultz, and Kleist 1969; Schultz and Asunmaa 1970). In analogy glycerophosphatide-galactosyldiglyceride complexes for the chloroplasts, tonoplast, and plasmalemma of plant cells will now be proposed. A variable aperture ion-gate is obtained by synchronized movement of the complex entities around an annulus of ordered water, stabilized by the polar ends of the phospholipid. It leaves a core of ordinary water open for ion transport.

The concept of salt-rejecting, ordered water was developed for submicroscopic pores of desalination membranes. Its validity in the various cell membranes and prototypes is tested by evidence from ultrastructural data and by supporting evidence from optics, phase diagram for the ternary system cholesterol-lecithin-water, and from NMR spectra available for membrane prototypes. References will be made to the indications of highly viscous, adsorbed water in cellulose and silica systems.

THE BINARY SYSTEM OF MACROMOLECULES AND WATER

The living cell consists of an intricate colloidal system of plasmagel and plasmasol in an aqueous medium. The system is not directly comparable to the hydrogels and hydrosols of inert colloids, whose binding forces are stationary under given thermo-

[1] Present address: McDonnell Douglas Astronautics Co., Western Division, Huntington Beach, California.

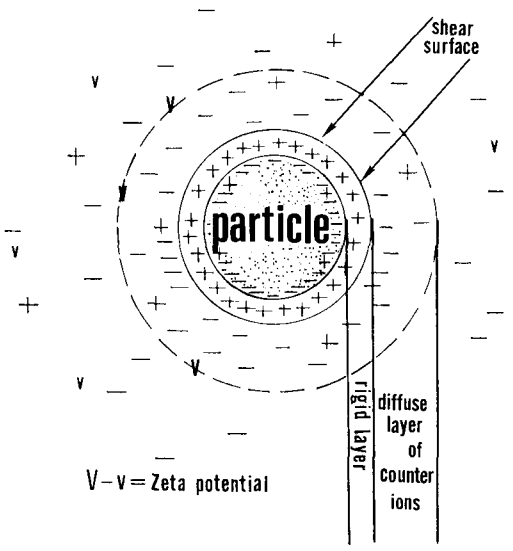

Fig. 1. Plane of shear around a charge-stabilized colloidal particle in aqueous solution.

dynamic conditions. A continuous change in cohesional binding and molecular adhesion by van der Waals forces and London dispersion forces provides the basis for living matter. The fluctuation is favored by the molecular heterogeneity of the cell organelles. Proteins, heteroproteins, nucleic acids, lipids, pigments, electrolytes, etc., cooperate.

Light scattering, or diffraction, is one of the measurable physical properties that clearly differentiate between the inert and the living colloids. The inert colloids with a supermolecular particle size show a Tyndall effect and a certain opacity in general. Some molecular dispersions of a short life time such as perfluorocarbon lauric acid in aqueous methanol are rare exceptions, according to experiments in the writer's laboratory.

The slightly bluish egg-white, on the other hand, suggests negligible light diffraction and lack of light scattering in spite of its specific gravity of over one g/cc. No actual Tyndall effect is observed. The difference in refractive indices in the medium and in the sol is compensated by the aqueous surface coating on the hydrosol. This adsorbed water may not be a monolayer. Additional evidence for the existence of an aqueous surface adsorbent is derived from two independent sources, namely, from hydrosol electrokinetics and from hydrophilic desalination membranes when immersed in an aqueous medium.

The electrokinetic properties, electrophoresis, of both inert colloids and fractions of the living system are well known. The Zeta potential around charge stabilized colloids provides a shear surface, isomorphic with the core particle, at some distance from the particle surface in the medium where the charge distribution profile shows a rapid change (Fig. 1). The Zeta potential is employed in paper technology for characterization of the various dispersed phases in white water, etc. Cellulose science and technology use the removal of the hydrosol water coating for precipitation fractionation of the gamma, beta, and alpha celluloses.

New evidence for the existence of a hydration sheath on hydrophilic surfaces when in contact with excess water was recently obtained from desalination processes in specially prepared cellulose acetate and porous glass membranes (Schultz et al. 1969; Schultz and Asunmaa 1970). The average pore size in both systems approximates 40–45 Å, dimensions too large for an ion-gate or for filtration of small organic or inorganic molecules. The high desalination efficiency of 98% and a reasonable water flux were explained by assignment of a mobile but salt-rejecting water layer on the hydrophilic surfaces. A schematic presentation of the ion filtration is shown in Fig. 2. Considering the maximum diameter of 8.4 Å of a hydrated sodium ion $Na(3H_2O)^+$, a water layer of some 18 to 22 Å is required for protecting the cylinder surface of the micropore and preventing the ion from entering the pore in reverse osmosis. If a salt-rejecting water closes the pore so that an opening, smaller than 8.4-Å but larger than 4-Å diameter remains for ordinary water, the $K(2H_2O)^+$-ion yet can be translocated. If both ions should be prevented from entering the micropore, the width of the core of ordinary water should be smaller than the minimum linear dimension of any of the hydrated ions to be rejected, and the pore diameter of the solid filter mate-

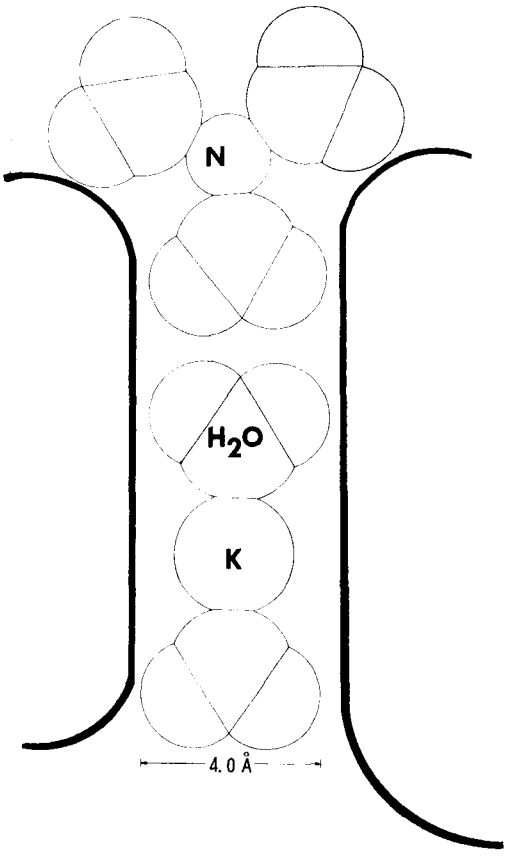

Fig. 2. Critical pore diameter for desalination by reverse osmosis. (For N read Na)

rial smaller respectively. The hydrated $K(2H_2O)^+$ is a water dipole, long and narrow. Since the filter pores are not of cylinder shape, Fig. 2 actually refers to the neck regions between pores.

The salt-rejecting water contains a higher number of hydrogen bonds per unit volume than ordinary water. It is therefore termed ordered water. It was computed (Schultz et al. 1969; Schultz and Asunmaa 1970) that the water clusters in the ordered water under the conditions of the desalination process contain 162 to 190 molecules. The physical properties, viscosity, etc., reported in the same reference are listed in Table 1. The data were computed from activation energies for the water flux at a practically constant desalination efficacy and from theoretical tortuosity, in the membrane pores.

We consider it very probable that the ordered water explains also an ion-gate in thin proteolipid membranes. A molecular model in Fig. 3 shows 18 units of lecithin-cholesterol binary complexes in a regular array surrounding a central pore so that the polar regions of the lecithin molecules are in contact with the pore water and the hydrocarbon chains occur extended toward the periphery of the assembly. It is suggested that a 21–22 Å-wide annular sheath of ordered water is lining the hydrophilic pore surface in analogy with the experiences from desalination membrane micropores. Again, the salt-rejecting water will leave a central opening of ordinary water as a core. It is suggested that the lecithin-cholesterol-water ternary system in Fig. 3 forms a membrane subunit. The subunit operates as a variable aperture since a synchronized movement of the binary complexes may shift the tilting angles slightly and cause an increase or decrease in the pore size. The size change is transmitted to the interior core of ordinary water, the proposed ion path, as well. Some mutual shift between two adjacent binary complexes and a potential bending of the hydrocarbon chain appear to complete the picture. The so-called

TABLE 1. *Physical properties of ordered water, adsorbed on a hydrophilic surface at 23 C*

t	= hydration sheath thickness (total)	= 21–22 Å
t_m	= hydration sheath thickness (mobile)	= 18–19 Å
d_{cl}	= average cluster diameter	= 21–22 Å
n_{cl}	= average cluster size	= 162–191 molecules
$\Delta H^{\ddagger}$	= activation enthalpy for flow	= 6.0–6.3 kcal/mole
$\Delta S^{\ddagger}$	= activation entropy for flow	= 5.6–6.5 cal/mole·°K
$\Delta F^{\ddagger}$	= free activation energy for flow	= 4.4 kcal/mole
ΔE_{vap}	= energy of vaporization	= 10.6–10.7 kcal/mole
η	= viscosity	= 0.35–0.37 poise

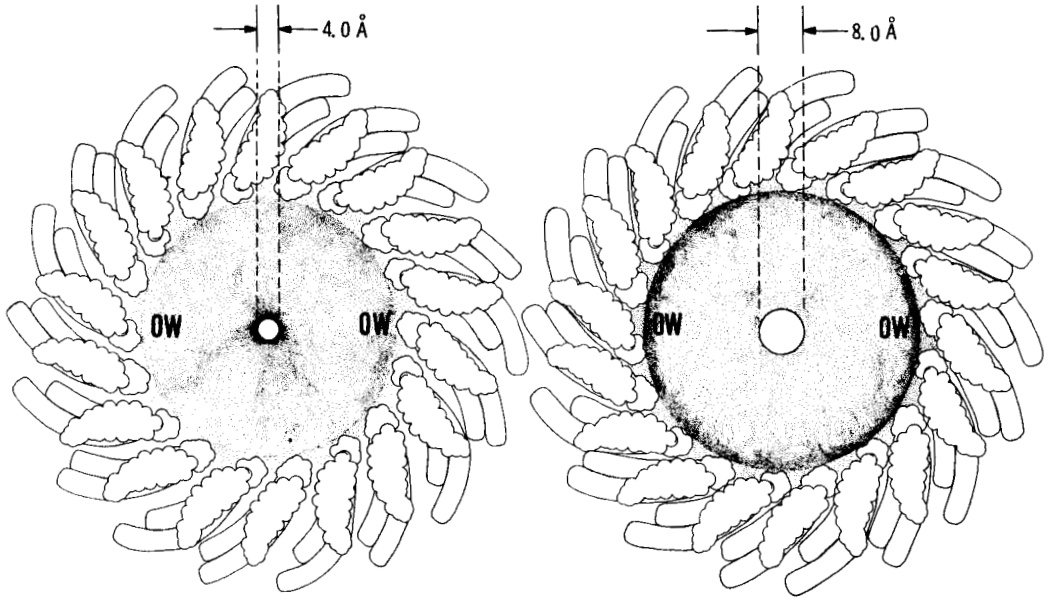

Fig. 3. Ion-gate membrane subunit; 18 cholesterol-lecithin binary complexes around an annulus *OW* of ordered water. The inner core diameter varies from 4 to 8.4 Å in the two open configurations. (Courtesy of Academic Press)

Vandenheuval projections (1963) were used for the cholesterol-lecithin assembly for improved accuracy rather than the molecular models of Stuart-Briegleb and photographs of them as common in stereochemistry. The Vandenheuval projection is the customary orthogonal projection in solid geometry. The sideview projection of the Vandenheuval cholesterol-lecithin complex was used as the first alternative (Fig. 4),

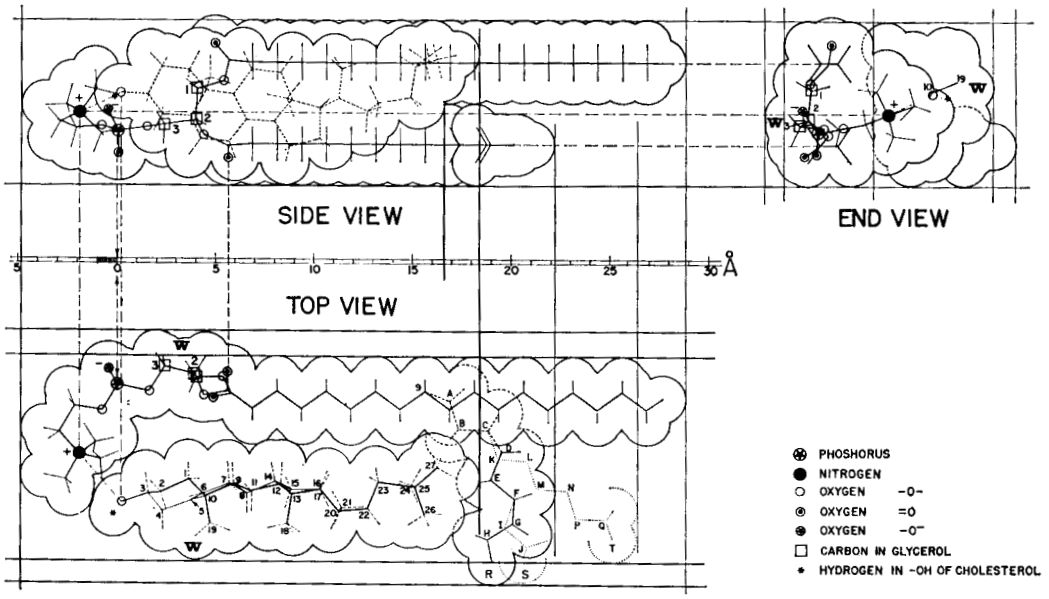

Fig. 4. Vandenheuval projection of a cholesterol-lecithin complex, side view designated A.

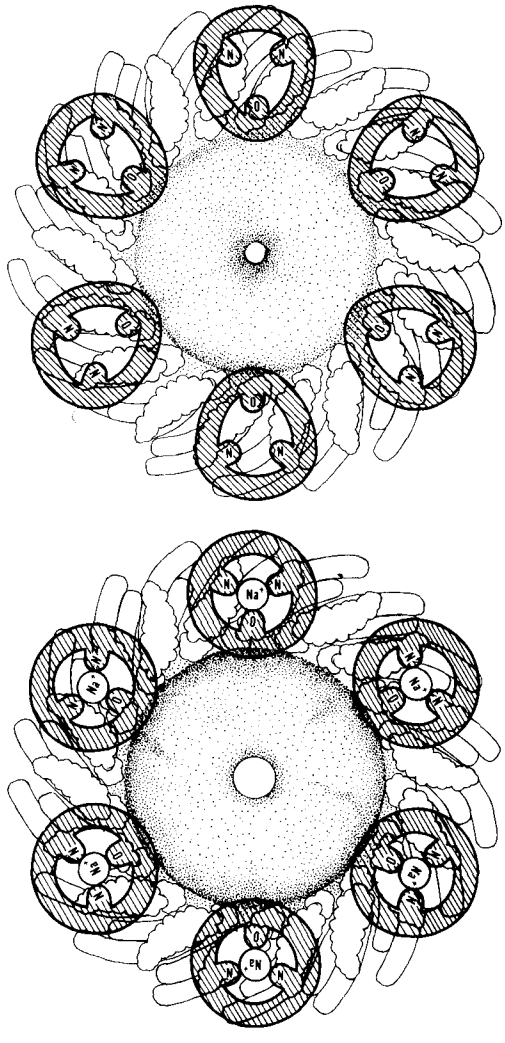

Fig. 5. Protein, absorbed on the annulus of cholesterol-phospholipids, provides a powering mechanism. Protein model the circular polypeptide alamethicin. (Courtesy of Academic Press)

since for a nonplanar molecule the adsorption may follow along any direction of the molecular axes.

The aperture size modification appears to be powered by surface adsorbed proteins (Schultz and Asunmaa 1970) according to Fig. 5. The molecular dimensions of the allosteric protein favor the adsorption. A relocation of the hydrophobic bonding between the adjacent subunits and the configuration change yield either increase or decrease of the size of the central core. The ion-gate diameter varies from 8.4 Å to 4 Å, the minimum dimension for transmission of the hydrated sodium and potassium ions. The ions enter the gate and diffuse through it under the influence of a Donnan potential or other external forces and a pumping action of the membrane structure due to reactions characteristic of active transport. In Fig. 6, a close-packing arrangement of the subunits from Fig. 3 is shown inducing a pattern designated "hexagonal" when examined at lower than molecular magnifications. The cholesterol-lecithin annulus in the subunit model (Fig. 3) is not symmetrical in polar coordinates; it is not a solid of revolution obtained by revolving an orthogonal projection *A* of the cholesterol-lecithin complex (Fig. 4) about an axis in its plane at a distance of 26 Å from its center. If considered a solid of revolution, the generating connected plane would be a cholesterol-lecithin complex projection at approximately 45°. This angle was chosen in model construction to obtain a close agreement with the dimensions of the actual membrane subunits of the suggested shape, observed in various preparations. The outer diameter of 105 Å is thus an experimental value. It yields an inner diameter that varies from 45 to 52 Å. The average thickness of the assembly will approximate 12 Å (Fig. 4) and may vary from 11 to 13 Å. The unsaturated chain on C_2 of glycerol in C_{15} lecithin can be either linolenic, linoleic, or oleic. Two of these 12-Å layers in superposition or adhered back-to-back will yield a membrane thickness of 24 Å that is roughly the thickness, 25 Å (Robertson 1964; 1965; 1966), of the middle layer of the plasma membrane in animal cells. It is consequently postulated that the hexagonal layer in Fig. 6 adheres back-to-back to its mirror image membrane to form a composite layer stabilized by lipid-lipid interaction in the contact zone. The actual membrane will finally be constructed of a laminated composite layer, protein-lipid-lipid-protein; *i.e.*, the protein adsorbing membrane subunits (Fig. 5) display the protein coat on both external surfaces of the membrane.

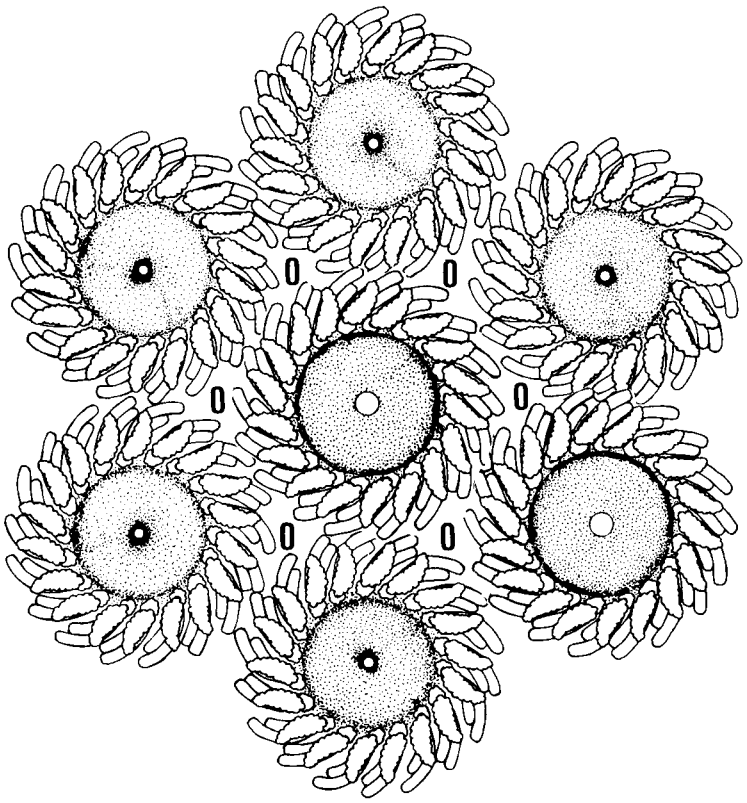

Fig. 6. The membrane subunits in hexagonal close-packing arrangement. Two units are shown in open configuration for $Na(3H_2O)^+$ translocation. The core opening in other subunits is 4 Å. Pores O are oleophilic.

CELL MEMBRANES WITH A SUBUNIT STRUCTURE

Most cell membranes when examined under an electron microscope in ultrathin sections of osmium-fixed tissue appear as two dark lines, separated by a nonosmiophilic zone. In some membranes this structure has been observed doubled, and globular units adhered to the "double membrane" appear to be characteristic of the enzyme-rich organelles (Sjöstrand 1953; Sjöstrand and Rhodin 1953). A new era in electron microscopy started when the osmium and methacrylate techniques were replaced by more nondestructive preparations such as the glutaraldehyde fixation in combination of ethylene glycol dehydrations.

Sjöstrand as early as 1963 suggested lipid globules stabilized between protein coats. Sjöstrand's recent electron micrographs (of mitochondrial membranes) reveal most delicate structures in molecular dimensions (Sjöstrand 1969; Sjöstrand and Barajas 1970). The detection of the actual basic membrane structure at the molecular level depends largely on preparation techniques. Proteins in animal cells, and the cell wall in plant cells may overshadow the lipid structure.

Glauert (1968) in a remarkable electron micrograph of the plasma membrane of the bacterium *Micrococcus radiodurans* shows the surface view in a negatively stained specimen (Fig. 7). Subunits, about 100-Å diameter, occur in a regular hexagonal pattern. A careful examination of the ultrastructure indicates electron opaque centers in the subunits. Overlapping of two membrane layers in a fold area produces an interesting Moiré magnification of the basic

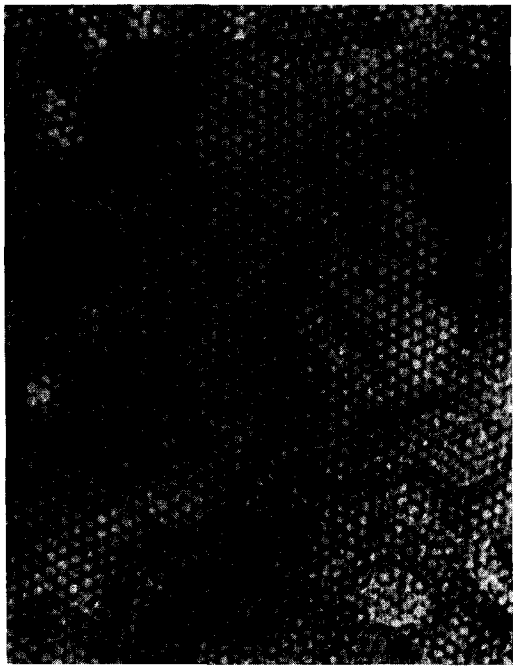

Fig. 7. A hexagonal pattern of subunits is shown in the plasma membrane of *Micrococcus radiodurans*. Note fold area with Moirè magnification. Electron micrograph by Glauert (1968).

entities. In the membrane cross section, the unit structure was hardly recognized. It is obvious that the *Micrococcus* structure supports the theory of the ion-gate mode. Similar structures were noted in Wehrmeyer's (Fig. 8) preparation of plastids of primary leaves of bean seedling in the 80,000-g sediment. Some preparation-induced dislocations are also shown. The 90-Å diameter subunits exhibit distinct negatively stained cores. The unit particles on lamellar fragments of the prolamellar body were isolated, using techniques where the stroma content was minimized (Wehrmeyer 1967).

Subunits of thylakoid membrane in *Aspidistra* granum in glutaraldehyde-$KMnO_4$ preparations were detected by Weier et al. (1965) in thin sections. The observed features were interpreted as sections of globular subunits with a light core, 37-Å diameter, and a dark rim, 28 Å wide, i.e., 93-Å diameter. Hohl and Hepton (1965) found similar units in the chloroplasts of fruitlets of immature pineapple fruit. The subunit dimensions were somewhat smaller, 75-Å diameter, the core 37 Å and the electron dense rim layer 20 Å wide.

A distinct cross striation (Fig. 9) in granal thylakoids from chloroplasts of spinach (*Spinacia*) leaves was demonstrated by Greenwood (1968) in ultrathin sections stained with uranyl acetate and lead citrate. Both heavy atom compounds induce an excellent negative staining and suggest ion-gates with center-to-center distances of 100 Å. A potential protein reaction requires further evaluation.

The subunit structure of phytoferritin, prepared from ribosomes of pea seedlings by Hyde, Hodge, and Birnstiel (1962) by salt gradient elution in ion exchange chromatography, shows striking similarity to the molecular model in Fig. 3. The subunit diameter was determined as 106 Å in Fig. 10.

An overall hexagonal subunit structure is suggested by electron micrographs of a partially degenerated wall of phage-infected *Vibrio fetus* membrane as noted by Ritchie and Bryner (1968). In a high resolution electron micrograph of the enzyme fractionated cell membrane, a hexagonal subunit array was depicted as shown in Fig. 11.

Similar features have been detected in other materials by Benedetti and Emmelot (1965, 1968) by Revel and Karnovsky (1967) in animal cells and recently by Hicks and Ketterer (1970) in isolated plasma membranes of the luminar surface of rat bladder epithelium. In unfixed samples, the center-to-center distances were as large as 140–150 Å, presumably because of weakening cohesion during preparation. Six 40-Å components were occasionally noted.

Another nondestructive solidification of the living cytoplasm is obtained by the freezing techniques, provided the formation of ice crystals is prevented by rapid cooling of water to the glassy state. The frozen etched samples display interesting fracture surfaces. Repeating units on the fracture face of the nonductile materials are quite correctly interpreted as a substructure of the frozen tissue rather than as a dimplar structure of the fracture mode.

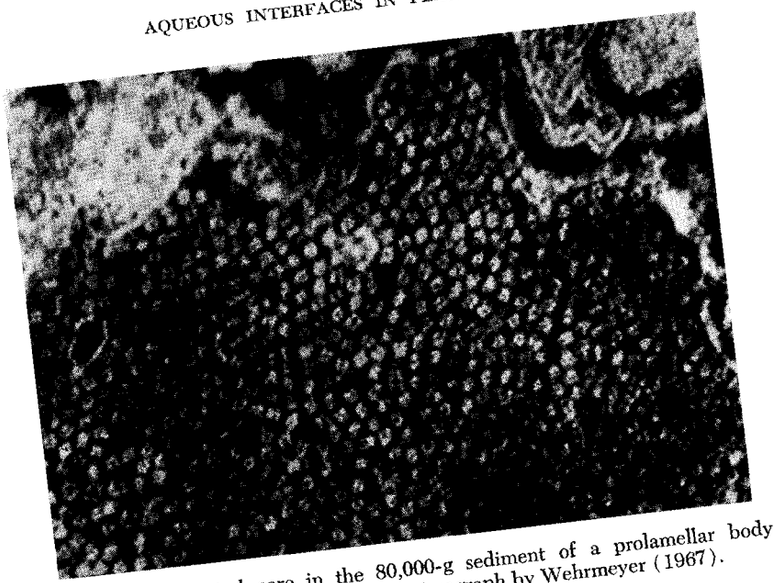

Fig. 8. Subunits with central core in the 80,000-g sediment of a prolamellar body preparation from plastids of leaves of bean seedlings. Electron micrograph by Wehrmeyer (1967).

Figure 12 shows an electron micrograph by Northcote (1968) of a replica of a frozen and etched plasmalemma from a pea (*Pisum*) root tip. The shallow depressions depict pit fields. A multitude of granules, 100- to 120-Å diameter, are noted. Similar features have been demonstrated by several research groups in various membranes (Moor and Mühlethaler 1965). The granules were originally explained as protein subunits, randomly distributed on the membrane surface. Recent observations indicate

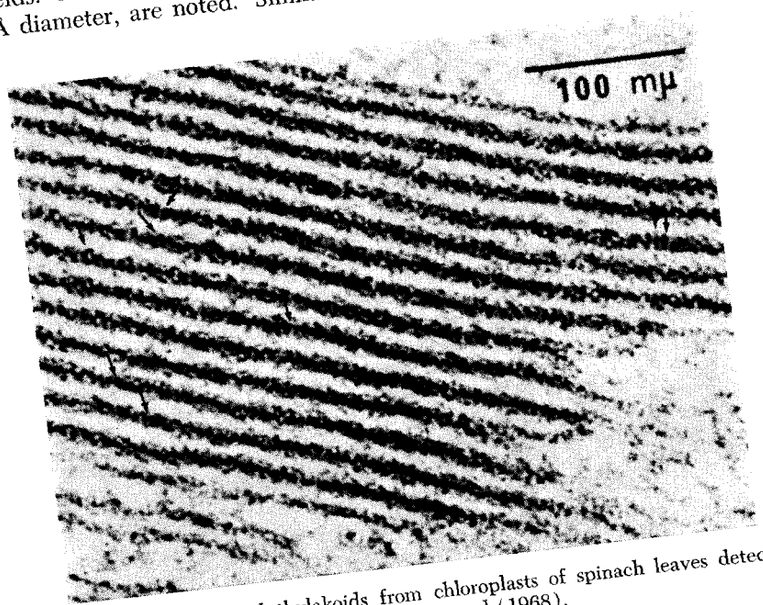

Fig. 9. Cross striation in granal thylakoids from chloroplasts of spinach leaves detected by (UO_2) and Pb ion staining. Electron micrograph by Greenwood (1968).

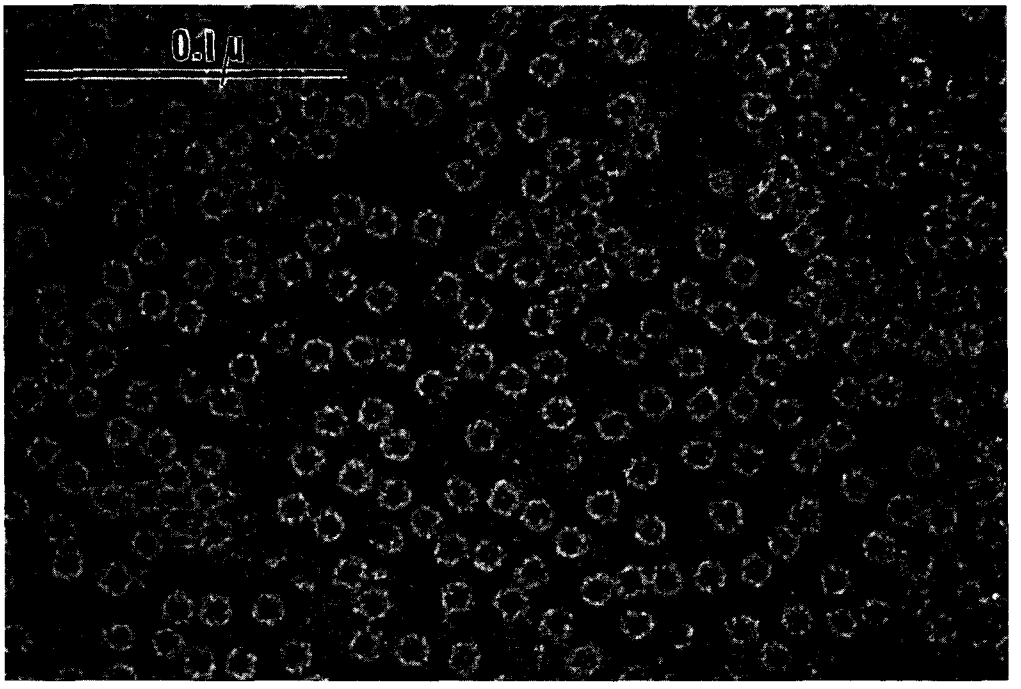

Fig. 10. Phytoferritin units, 106-Å diameter, show an annulus shape. Electron micrograph by Hyde, Hodge, and Birnstiel (1962).

that the membrane frequently is split along the middle zone in preparation (Pinto da Silva and Branton 1970). We consider it therefore very probable that the fracture path may transfer from one membrane unit plane to the adjacent one, especially if variations in the local cohesional strength occur. Occasionally the lipid-lipid interaction in the membrane plane between subunits may not be as strong as the lipid-lipid interaction between the two component membranes. A weakly bound subunit under these circumstances will remain adhered to a similar subunit above. A differential thermal contraction of the plasmasol components under the rapid freezing may facilitate the suggested weakening of bond strength. The structures revealed in frozen etched membranes therefore may imply the ion-gate subunit structure rather than a heterogeneous enzyme protein distribution. We recall that the ion-gate model suggests dimensional congruity in the contact plane between the phospholipid annulus and the surface adhered protein, as discussed in Fig. 5.

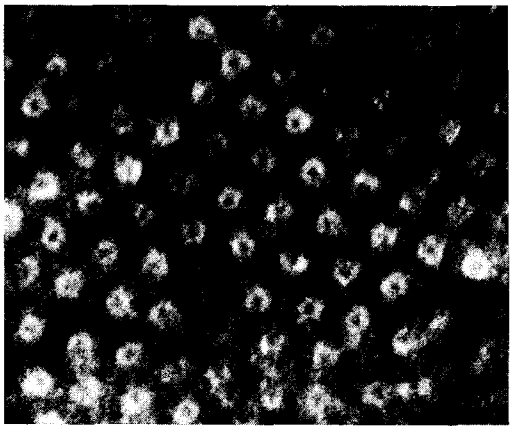

Fig. 11. Hexagonal array of unstained regions with central core is depicted in phage infected *Vibrio fetus* membrane. Electron micrograph by Ritchie and Bryner (1968).

LIPIDS IN CHLOROPLASTS

For construction of a proteolipid ion-gate model for plant cells, the close-packed arrangement of subunits in a developing

Fig. 12. Replica of frozen etched membrane of plasmalemma of root tip of pea (*Pisum*) displays surface elevations, 100–120 Å wide. Electron micrograph by Northcote (1968).

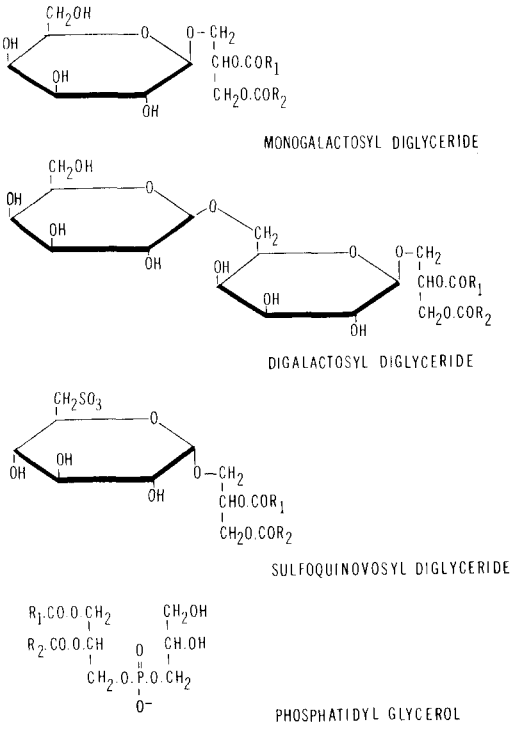

Fig. 13. Chloroplast lipids.

membrane from the prolamellar body (Fig. 8) is selected as a prototype, since the chemistry and biochemistry of the chloroplast lipids are rather well established.

The chloroplast lipids contain 10% glycerophosphatides, 40% glycolipids, and 50% of a combination of sulfolipids, pigments, etc. (Nichols and James 1968). The hydroxyl-rich glycerophosphatid, the equally hydroxyl-rich mono- and diagalactosyldiglycerides, and the sulfoquinovosyl diglyceride are the four major lipid components. Lecithin occurs in very small quantities, presumably as an impurity. The chain length of the lipid fatty acids varies from lipid to lipid and as a function of light exposure. The maximum number of double bonds per chain is three in the photosynthetic tissue. The 18:3 fraction in the galactosyldiglycerides varies from 37 (di) to 45% (mono), as compared with 4 to 5% in the etiolated material. The sulfolipid composition remains surprisingly constant. Chemical analysis thus indicates that the monogalactosyl glyceride and the phosphatidyl glycerol are the most active lipids in photosynthesis. They also participate in galactose and phosphate metabolism, respectively. These two lipids were selected as basic components for the model of the prolamellar membrane.

For construction of the ion-gate model, the stereochemical lipid structures are compared in Fig. 13. The phosphatidyl glycerol in its stereochemistry is very similar to lecithin. The lecithin NH_2^+ radical is substituted for the nonesterified part of the glycerol, which provides two free hydroxyls for bonding. The polar region thus extends from the phosphorylation site to the end hydroxyls. The acid radicals have been found to consist of 31% C_{16} fatty acids, designated (16:0), 16% C_{16} with one double bond designated (16:1), 10% (18:1), and 25% (18:2). Since over 50% consist of C_{16}, we employ this shorter chain for the model construction. The two units (CH_2) decrease the chain length by 2.54 Å on each side of the membrane subunit model. The subunit diameter in this system will thus approximate 90 Å, in good agreement with the values measured from the electron micrographs.

The monogalactosyldiglyceride stereostructure indicates the same proximity of the hydrocarbon chains as was noted in lecithin. It also shows the same chain length of 18C. The difference in molecular width in cholesterol and the chloroplast lipids is compared in Fig. 14. A close-packing of the hydrocarbon chains will result in an annulus constructed of 27 galactosyldiglyceride units. Hydrogen bonds are formed between the adjacent galactose units via hydroxyls at short separation. This means increased rigidity in the subunit, and finally less selective permeability. These are properties known for the tonoplast and the plasmalemma, which probably also contain an essential amount of the galactosyldiglycerides and other polar lipids.

SUPPORTING EVIDENCE FROM PHYSICAL CHEMISTRY OF NATURAL MEMBRANES

The nonpolar character of the cell membrane was concluded in early experiments on permeability of plant protoplasts (Briggs, Hope, and Robertson 1961). The permea-

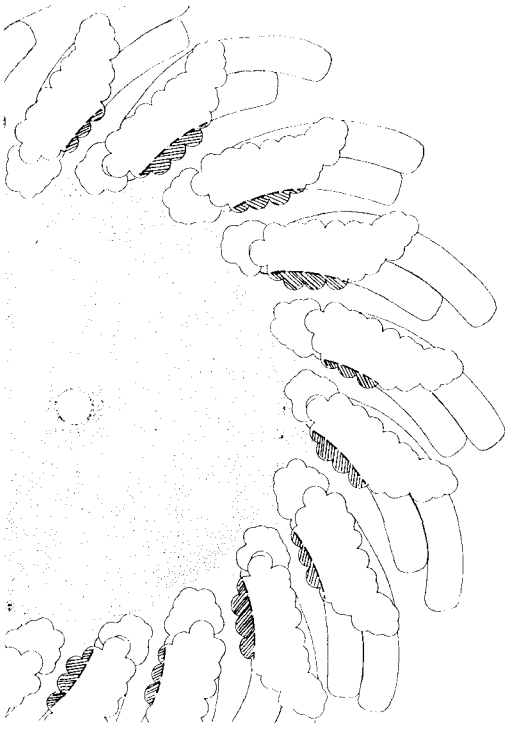

Fig. 14. Close-packing of chloroplast lipids compared with the cholesterol-lecithin annulus.

bility rate of oleophilic, nonpolar molecules appeared significantly higher than that of water soluble substances, when measured for hypertonic solutions. In the ion-gate model in Fig. 4, the areas display oleophilic pores with hydrocarbon peripheries and provide a passageway for oleophilic substances, especially under hypertonic conditions, when the surface proteins may be deformed to enlarge the spacing between adjacent membrane subunits and block the ion-gate.

Sjöstrand in a recent review of permeability of plasma membranes (1969) concludes that separation of ion-accessible pores will approximate 100 Å during activation of squid axon. Similarly Parpart and Ballentine (1952) and Parpart and Hoffman (1954) have estimated the number of micropores per unit area in cellular membranes and suggest one pore per 10^4 square angstrom.

The ion-gate membrane subunit model (Fig. 4) displays center-to-center distances that vary from 90 to 110 Å, depending on the molecular length of the lipid involved. The agreement is excellent. The surface area per pore is 7,800 $Å^2$ for a 90-Å unit, 11,000 for a 120-Å unit and varies mainly between 8,000 and 9,000 square angstrom.

Among the well-established characteristics of natural membranes, Briggs, Hope, and Robertson (1961) tabulate among electrical and permeation properties the very low surface tension and high flow rate of water. The surface tension of 0.1 to 1 dyne cm^{-1} is 60 to 6 times lower than the lowest value measured for perfluorocarbon surfaces consisting mainly of the CF_3 radical, which is known for its extremely low specific surface free energy 6 dyne cm^{-1}. Lower values have been measured only for proteins with an electric surface charge. The measurements for the plasma membrane were made both on the exterior surface and on the inside of a mackerel egg (Frey-Wyssling and Mühlethaler 1960). The ion-gate model of the membrane subunit proposes a back-to-back assembly of two subunits with protein attachments on both exterior surfaces; the inside as well as the outside surfaces of the mackerel egg consequently will display mainly proteinaceous surfaces.

The high flow rate of water is also explained by the ion-gate model. The high water flux in desalination processes suggested that the ordered water flows freely along the pore surface but is not capable of dissolving ions or molecules. The water flux in desalination processes was measured under pressures of 1,500 psi. Experimental flow rate ratio of 550 has been determined for plant cells (Briggs, Hope, and Robertson 1961) where a water permeability of 0.02 cm/sec was measured but a value of 1.1×10^{-6} cm/sec was found as urea flux.

Repeated references are made in literature to lipid extraction that does not destroy the membrane in spite of removal of 70% of the lipids (Frey-Wyssling and Mühlethaler 1960). The extent of destruction was concluded from electron micrographs of osmium-fixed material. The membrane laminate protein-lipid-lipid-protein of two ion-gate subunits in superposition offers an interpretation. The protein cover in Fig. 5

Fig. 15. Condensed phases in stearic acid film on water surface are shown as circular areas. Electron micrograph by H. E. Ries, Jr. (1961).

suggests that a lipid extraction results in removal of the membrane interior and a protein residue remains in place as membrane exterior surfaces. The protein envelope does not collapse, if the proteins are denaturated or fixed *in situ*. The resolution obtained in electron micrographs may not always suffice for detecting a missing lipid component between the proteinaceous exterior surfaces since the membrane thickness remains unchanged.

The vacuolar membrane tonoplast is rich in polar lipids. The lipids appear to exist as liquid crystals since electrolyte addition may detach the lipids from their original arrays and rearrange them on the aqueous surface as myelin figures (Frey-Wyssling and Mühlethaler 1960).

So far most membrane characteristics reported but not explained in the vast amount of experimental data available are in favor of the ion-gate model.

THIN PROTEOLIPID MEMBRANES *IN VITRO*

Lyotropic paracrystalline phases are obtained in ternary systems of amphiphilic substances in aqueous environments.

Phase changes in a stearic acid film on the chemically inert water surface are shown in Fig. 15. Circular islands represent the condensed phase, which maintains the intermittent region under a degree of compression. When the pressure increases to exceed an equilibrium value of the two-dimensional condensed phase, this phase

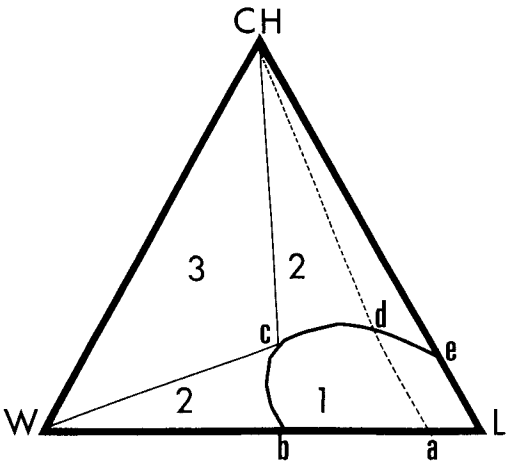

Fig. 16. Phase diagram for the ternary system cholesterol-lecithin-water by Small and Bourgés. Number of phases present are marked 1, 2, 3. Region *a d e L* not analyzed.

will continue to grow until a complete monolayer is formed. As a prephase, nucleation is observed in the areas between islands. Formation of a condensate is favored by a strong interaction between adsorbate and the adsorbent and by an adsorption heat that exceeds the condensation heat (Hudson and Ross 1965).

Phase diagram for the ternary system of cholesterol-lecithin-water under constant thermodynamic conditions (Fig. 16) has been published by Small and Bourgès (1965). Areas where 1, 2 or 3 phases were observed are indicated. Mixtures containing 12–45% water form a lamellar liquid crystalline phase, detected as myelin figures. Increase of water content induces a phase growth observed as a floating surface film. The film also consists mainly of so-called myelin features, which have been frequently illustrated in electron micrographs (Glauert,

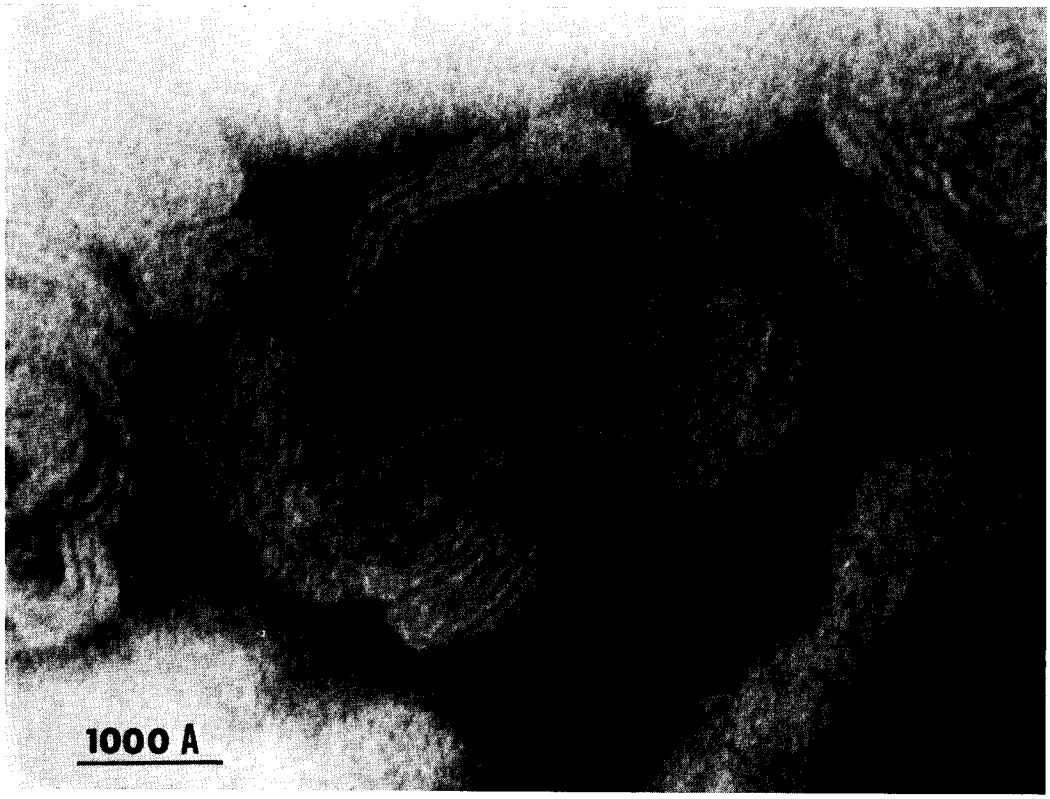

Fig. 17. Myelin figures and thin discs with central cores form the two phases present in an artificial proteolipid membrane of squalene-lecithin.

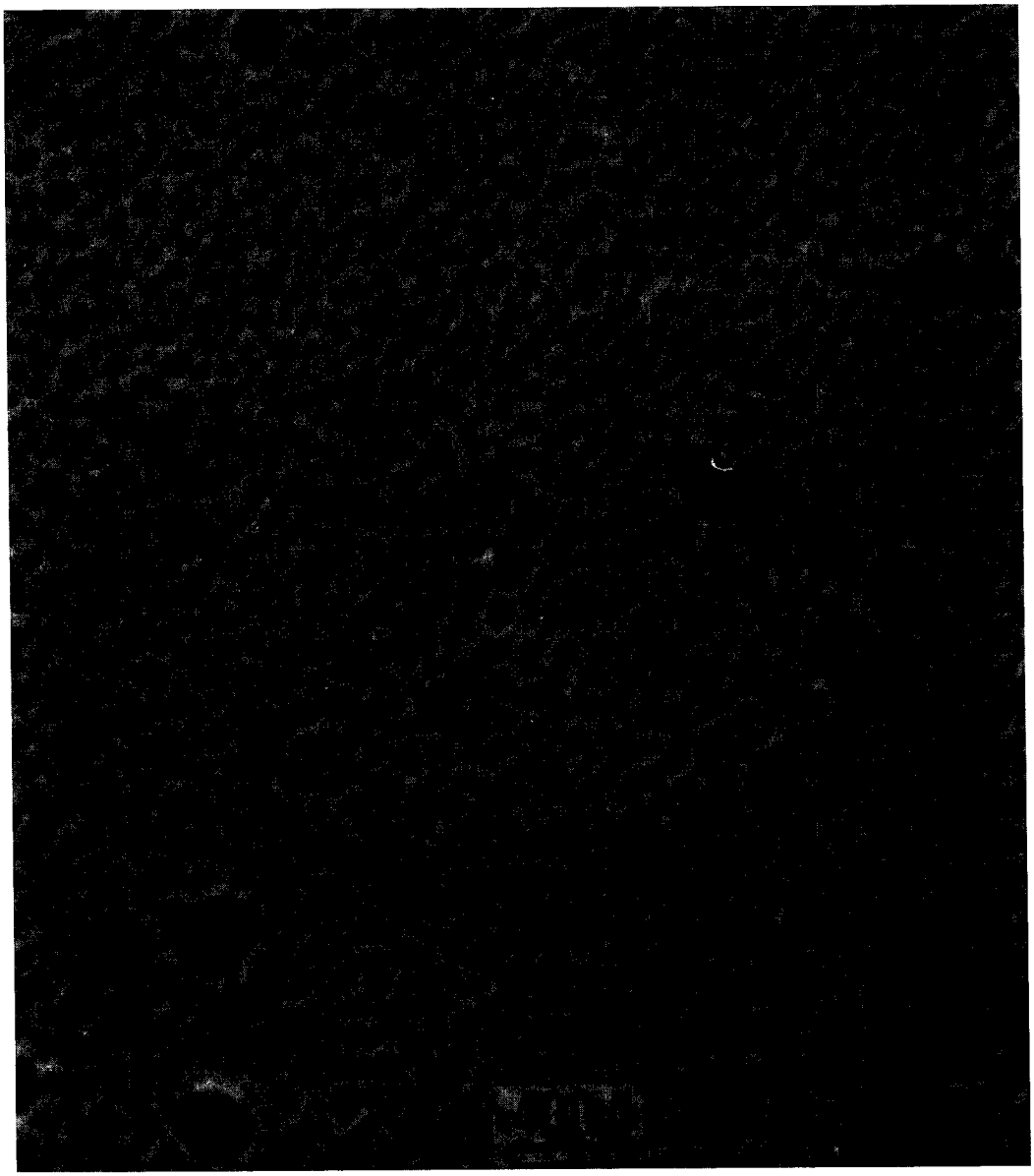

FIG. 18. An ultrathin proteolipid membrane of squalene-lecithin (stabilized by protamine) displays the micelle phase in hexagonal close-packing. Excess stain marked S.

Dingle, and Lucy 1962; Junger and Reinauer 1969). Figure 17 from our collections shows the myelin structure in a film of protein stabilized lecithin. Concentric cylinders of the lamellar liquid crystalline phases are shown with a decreasing cylinder diameter. The X-ray d-spacing of 50 Å is characteristic of this phase.

With increasing water content, Small and Bourgès observed a beginning turbidity and an increasing d-spacing up to 65 Å. The lecithin-water ratio can be calculated, assuming that the water is connected with the polar ends of the lipids and assuming a density of 1.0 also for lecithin. The d-spacing change indicates a decrease in the lipid

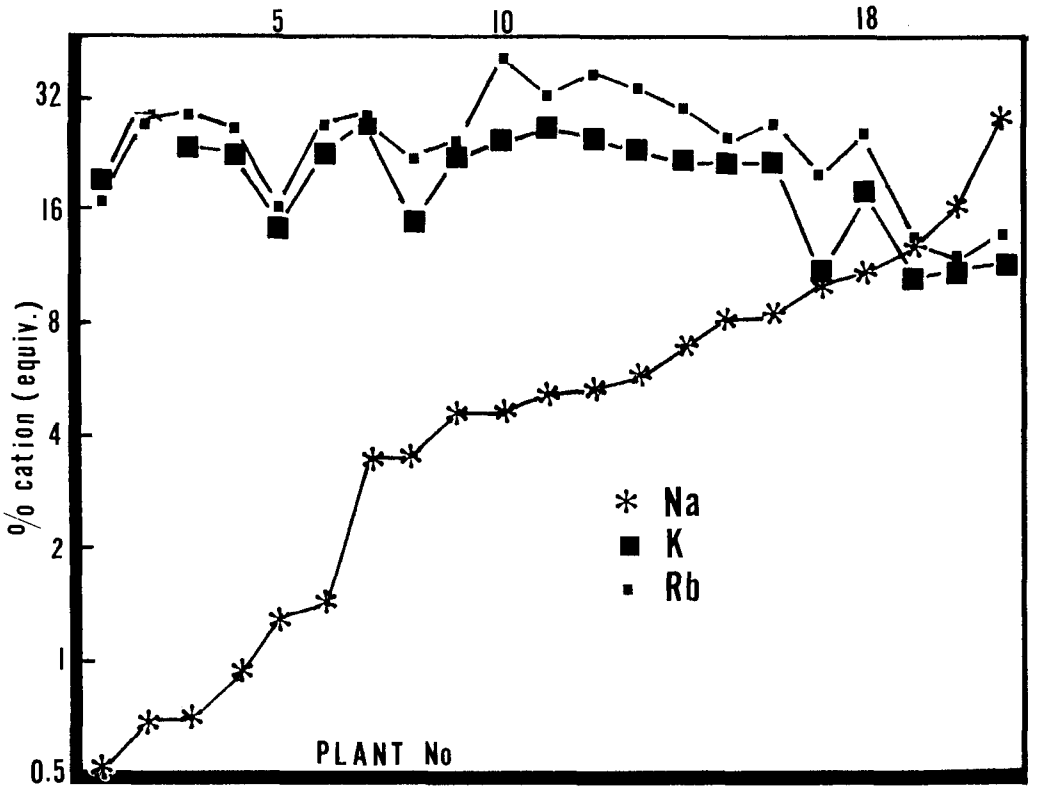

Fig. 19. Variations in diffusion rate of Na, K, and Rb ions in plants numbered 1 through 21 indicate differences in permeability. (Courtesy of Blackwell Scientific Publ. Co.)

layer thickness with increasing lecithin hydration. The average molecular contact area at the water interface consequently increases. At the stage of extended hydration, the lecithin does not contact water at its polar end exclusively as in the primary phase when the contact area approximates the molecular cross section 18.2 Å^2. The amphiphilic character is displayed, especially in the cholesterol-lecithin complex. The lamellar paracrystalline phase is transformed to liquid crystals where the hydrated lecithin or the hydrated lecithin-cholesterol complex acquires a maximum contact area with water. The cholesterol hydroxyl is hydrophilic and attracts the oleophilic complex to the surface plane of water. The cholesterol unit is interdigitated above the lecithin hydrocarbon leaflets (in the membrane subunit model in Fig. 3); the hydroxyl attraction thus mobilizes the entire complex. Liquid crystalline phases are obtained with a cylinder packing, a pile up of Fig. 3 models, noted as micelles. The micelle distribution is a function of water content. Micelle compacts may form either face centered cubic or hexagonal close-packed arrays, termed paracrystals. Nuclear magnetic resonance studied by Lawson and Flautt (1965) confirm the results.

The close-packed, annulus type paracrystalline phases with a minimum cylinder length are shown in our electron micrographs of thin proteolipid membranes (Fig. 18), stained with sodium phosphotungstate. The dimensional agreement with the membrane subunits with those observed in living cells is unique. Details of the film preparation have been published elsewhere.

COMMENTS

In the extensive literature (Drost-Hansen 1969) on the structure and properties of water adsorbed on solid surfaces, a few

experimental data appear of specific interest for the discussion of plant cells.

Solid-water interaction (Mysels 1966) and the existence of a "specific" water (Fowkes 1966) in hydrocarbons saturated by water, are concluded from the spread of the freezing point over a region from –15 to –30 C (Mysels 1966). Structural water on hydrophilic materials such as cellulose, hemicellulose, clay, silica, and glass has been suggested by a variety of property anomalies. The presence of anomalous water on cellulose samples was inferred by Kubát and Pattyranie (1967) from the abrupt changes in the temperature dependence of mechanical damping at +35 and –30 C. The latter anomaly region was verified by Ramiah and Goring (1965) by dilatometric analysis of thermal expansion of water-swollen cellulose and hemicellulose preparations.

A water coating, six monolayers thick, on glass surfaces was computed by Kawasaki, Kanov, and Sakita (1958) from conductivity data; and water structures, different from that of ice below the freezing point were proposed by Wu (1964) on clay as an interpretation of NMR spectra.

If the concept of ordered water in the ion-gate model proves to be correct, as strongly suggested by a set of experimental observations, a new field of interdisciplinary effort calls for characterization of the binary and ternary systems of lipids, proteins and water, both *in vivo* and *in vitro*.

Significant variations in the ion diffusion rates in a variety of plants as shown in Fig. 19 (Collander 1941) imply that the ion-gate will not be the only governing parameter in the integral system of electrolyte transport in living plants.

The compact structure of the mitochondrial membranes revealed in the superb electron micrographs by Sjöstrand (Sjöstrand 1969; Sjöstrand and Barajas 1970) implies that the ion-gate model should not replace the previous concept of "unit membrane" *a piori*. Its validity should be tested for systems where appropriate preparations will facilitate an electron microscopic analysis of this suggested membrane component.

REFERENCES

Asunmaa, S. K., R. D. Schultz, and F. D. Kleist. 1969. Ultrastructure of thin proteolipid membranes. *In* C. J. Arceneaux (ed.), Proceedings 27th Annual Meeting, Electron Microscopy Soc. of America. St. Paul, Minn., Aug. 26–29, 1969, Claitor's Publishing Division, Baton Rouge, La., p. 336.

Benedetti, E. L., and P. E. Emmelot. 1965. Electron microscopic observation of negatively stained plasma membranes isolated from rat liver. J. Cell Biol., **26**: 299.

———, and ———. 1968. Hexagonal array of subunits in tight junctions separated from isolated rat liver plasma membranes. J. Cell Biol., **38**: 15.

Briggs, G. E., A. Hope, and R. N. Robertson. 1961. Electrolytes and plant cells, v. 1. Botanical Monographs, F. A. Davis Company, Philadelphia, Pa. Blackwell Scientific Publ. Co., Oxford.

Collander, R. 1941. Selective absorption of cations by higher plants. Plant Physiol., **16**.

Drost-Hansen, W. 1969. Structure of water near solid interfaces. Ind. Eng. Chem., **61**(11): 10.

Fowkes, F. M. 1966. Part of general discussion on colloid stability in aqueous and nonaqueous media. Faraday Soc. Disc., **42**: 140.

Frey-Wyssling, and K. Mühlethaler. 1960. Ultrastructural plant cytology. Elsevier Publ. Co., Amsterdam, London, N. Y., p. 145.

Glauert, A. M. 1966. Moiré pattern in electron micrographs of a bacteria membrane. J. Cell. Sci., **1**: 425.

———, N. T. Dingle, and J. A. Lucy. 1962. Action of saponin on biological cell membranes. Nature, **196**: 952, 953.

Greenwood, A. D. 1968. *In* J. H. Burnett (ed.), Plant cells by F. A. L. Clowes and B. E. Juniper, v. 8, Botanical Monographs, Blackwell Scientific Publ. Co., Oxford, p. 135.

Hicks, R. M., and B. Ketterer. 1970. Isolation of the plasma membrane of the luminal surface of rat bladder epithelium and the occurrence of a hexagonal lattice of subunits both in negatively stained whole mounts and in sectioned membranes. J. Cell Biol., **45**: 542.

Hohl, H. R., and A. Hepton. 1965. A globular subunit pattern in plastid membranes. J. Ultrastruct. Res., **12**: 542.

Hudson, J. B., and S. Ross. 1965. Adsorption and condensation processes. *In* D. E. Gushee (ed.), Chemistry and physics of interfaces, reprinted from Industrial and Engineering Chemistry, Sept. 1964–Sept. 1965, American Chemical Soc. Publications, Washington, D.C., p. 103.

Hyde, B. B., A. J. Hodge, and M. L. Birnstiel. 1962. Phytoferritin: A plant protein discovered by electron microscopy. *In* S. S. Breese (ed.), Proceedings 5th International

Congress for Electron Microscopy, Philadelphia, Pa., Academic Press, v. 2, T 1.

JUNGER, E., AND H. REINAUER. 1969. Liquid crystalline phases of hydrated phosphatidyl ethanolamine. Biochem. Biophys. Acta, **183:** 304.

KAWASAKI, K., K. KANOU, AND Y. SAKITA. 1958. Liquid-like layers in the adsorbed film of H_2O on glass. J. Phys. Soc. Japan, **13:** 222.

KUBÁT, J., AND C. PATTYRANIE. 1967. Transition in cellulose in the vicinity of −30 C. Nature, **215:** 390.

LAWSON, K. D., AND T. J. FLAUTT. 1965. Nuclear magnetic resonance studies of surfactant mesophases, presented at Internatl. Liquid Crystal Conference, Kent State Univ., Ohio, 1965, Aug. 15–20. Publ. *In* C. J. Diene and M. M. Labes (eds.), Molecular crystals (1966), **1** (2): 24.

MOOR, H., AND K. MÜHLETHALER. 1965. *In* Ultrastructural plant cytology by A. Frey-Wyssling and K. Mühlethaler. Elsevier Publ. Co., Amsterdam, London, N. Y., p. 148, 170, 184, 186, 264.

MYSELS, K. J. 1966. Part of general discussion on colloid stability in aqueous and nonaqueous media. Faraday Soc. Disc., **42:** 138.

NORTHCOTE, D. H. 1968. *In* J. H. Burnett (ed.), v. 8, Plant cells by F. A. L. Clowes and B. E. Juniper. Botanical Monographs. Blackwell Scientific Publ. Co., Oxford, p. 260.

NICHOLS, B. W., AND A. T. JAMES. 1968. The function and metabolism of fatty acids and acyl lipids in chloroplasts. *In* J. B. Pridham (ed.), Plant cells. Academic Press, N. Y., p. 163.

PARPART, A. K., AND J. F. HOFFMAN. 1954. *In* H. T. Clark (ed.), Ion transport across membranes. Academic Press, N. Y., p. 69.

———, AND R. BALLENTINE. 1952. *In* E. S. B. Barrow (ed.), Modern trends in physiology and biochemistry. Academic Press, N. Y., p. 135.

PINTO DA SILVA, P., AND D. BRANTON. 1970. Membrane splitting in freeze-etching, covalently bound ferritin as a membrane marker. J. Cell Biol., **45:** 598.

RAMIAH, M. V., AND D. A. I. GORING. 1965. The thermal expansion of cellulose, hemicellulose and lignin. J. Polymer Sci., Pt. C No. 11; 27.

REVEL, J. P., AND M. J. KARNOVSKY. 1967. Hexagonal array of subunits in intercellular junctions of the mouse heart and liver. J. Cell Biol., **33:** C7–C12 (following p. 450).

RIES, H. E., JR. 1961. Monomolecular films. Scientific Am., **204:** 152

RITCHIE, A. E., AND J. H. BRYNER. 1968. A structural element in the envelope system of *Vibrio fetus*. *In* C. J. Arceneaux (ed.), Proceedings 26th Annual Meeting, Electron Microscopy Society of America, New Orleans, La., 1–9 Sept. 1968. Claitor's Publishing Division, Baton Rouge, La., p. 78.

ROBERTSON, J. D. 1966. Current problems of unit membrane structure and contact relationships. *In* Proceedings of Conference on Nerve as a Tissue, Philadelphia, Pa., 12–13 Nov. 1964. Harper and Row, Publishers, N. Y., London, p. 11–48.

———. 1966. Granulo-fibrillar and globular substructure in unit membranes (electron microscopy). New York Academy of Sciences, **137** (2): 421.

———. 1965. Design principles of the (animal cell) unit membrane. *In* CIBA Foundation Symposium on principles of biomolecular organization 9–11 June 1965. London; Little Brown and Company, Boston 1966, p. 357.

SCHULTZ, R. D., AND S. K. ASUNMAA. 1970. Ordered water and the ultrastructure of the cellular plasma membrane. *In* J. F. Danielli, A. C. Riddiford, and M. D. Rosenberg (eds.), Recent progress in surface science, v. 3, Academic Press, N. Y., p. 291.

———, ———, AND F. D. KLEIST. 1969. Ultrastructure and variable aperture pore function of hexagonal subunits in plasma membranes, Paper 10246 McDonnell Douglas Co., Newport Beach, Calif., presented at the 2nd Internatl. Meeting of the Internatl. Society of Neurochemistry, Milan, Italy, 1–5 Sept. 1969.

———, ———, G. A. GUTER, AND F. E. LITTMAN. 1969. Characterization of ordered water in hydrophilic membrane pores, Paper 10247 McDonnell Douglas Co., Newport Beach, Calif., presented at the 2nd Internatl. Meeting of the Internatl. Society of Neurochemistry, Milan, Italy, 1–5 Sept. 1969.

SJÖSTRAND, F. S. 1953. The ultrastructural organization of retinal rods and cones. *In* Proceedings of the Annual Meeting of the Electron Microscopy Soc. of America in Cleveland, Ohio, 6–8 Nov. 1952. J. Appl. Phys. 1953, **24:** 117.

———. 1962. Molecular architecture of cell membrane and cytoplasmic membranes. *In* Proceedings Internatl. Pharmacology Meeting in Stockholm, 1961, v. 4, p. 1. (Publ. 1962.)

———. 1963. A comparison of plasma membrane, cytomembranes and mitochondrial membrane elements with respect to ultrastructural features. J. Ultrastruct. Res., **9:** 561.

———. 1963. A new repeat structural element of mitochondrial and certain cytoplasmic membranes. Nature, **199:** 1262.

———. 1963. A new ultrastructural element of the membranes in mitochondrial and some cytoplasmic membranes. J. Ultrastruct. Res., **9:** 340.

———. 1969. Morphological aspects of lipoprotein structures. *In* E. Tria and A. M. Scanu (eds.), Structural and functional aspects of

lipoprotein structures in living systems. Academic Press, N. Y., p. 73.

———. AND L. BARAJAS. 1970. A new model for mitochondrial membranes based on structural and biochemical information. J. Ultrastructure Research. In press.

———, AND J. RHODIN. 1953. The ultrastructure of the proximal convoluted tubules of the mouse kidney as revealed by high resolution electron microscopy. Exp. Cell Res., **4**: 426.

SMALL, D. M., AND M. BOURGÈS. 1965. Lyotropic paracrystalline phases obtained with ternary and quarternary systems of amphiphilic substances in water: Studies on aqueous systems of lecithin, bile salt and cholesterol. *In* G. H. Brown, G. J. Dienes, and M. M. Labes (eds.), Liquid crystals. Proceedings Internatl. Conference on Liquid Crystals, Kent State Univ., Ohio, 16–20 Aug., Gordon and Breach, Science Publishers Inc., N. Y., p. 221.

VANDENHEUVAL, F. A. 1963. Biological structure at the molecular level with stereomodel projections; I, The lipids in the myelin sheath of nerve. J. Am. Oil Chemists' Soc., **40**(9): 455.

WEIHRMEYER, O. 1967. Prolamellar bodies, structure and development. *In* C. Sironval (ed.), Le Chloroplaste, Croissance et Vieillissement. Masson et C^ie^ Editeurs, Paris, p. 62.

WEIER, T. E., A. H. ENGELBRECHT, A. HARRISON, AND E. B. RISLEY. 1965. Subunits in the membranes of chloroplasts of *Phaseolus vulgaris*, *Pisum sativum*, and *Aspidistra* sp. J. Ultrastruct. Res., **13**: 92 and *In* J. T. O. Kirk and R. A. Tilney-Basset (eds.), The plastids. W. H. Freeman and Co., London, San Francisco, p. 48.

WU, T. H. 1964. A nuclear magnetic resonance study of water in clay. J. Geophys. Res., **69**: 1083.

KACALIN, N. V. 1969. Heating of veneer flitches in autoclaves. *Naučnye Trudy Leningradskoj Lesotexničeskoj Akademij* 138: 62–67. (Russian, no English abstract). When veneer flitches are heated as preparation for veneer cutting, growth stresses and shrinkage cause the ends to check. The flitches dry and shrink also during heat treatments in autoclaves. In the heating-up period, wood loses some moisture until the atmosphere in the autoclave is saturated. The material dries rapidly at the end of the treatment when the pressure of 110 to 150 psi is released and the steam becomes superheated. The hot flitches continue to dry after the autoclave is opened. By adding water to the autoclave's base and slowly releasing the pressure within two hours at the end of the treatment, the length of end checks in 63 ash flitches increased by 21% during the treatment, whereas the average check length of 86 controls in usual autoclave treatments increased by 38%. Similar results were achieved with larch flitches. (H.K.)

KÜRSCHNER, K. 1969. On some obstinate aberrations in wood chemistry. *Holztechnologie* 10(3):161–167(G.gre). This is a discussion of literature and research results on the extraction of vanillin from wood. (R.E.)

LEONOVIČ, A. A. AND N. J. SOLEČNIK. 1969. On the production technology and characteristics of fire-resisting fiberboards. *Holztechnologie* 10(4):219–224(G.gre). The fire characteristics of newly developed fire-resistant fiberboards are demonstrated under ignition conditions: reducing the commencement of active pyrolysis and the amount of volatiles generated with it; reducing the amount of heat liberated because of exothermic reactions. The lowering of temperature and pressure with pressing process is explained, reference is made to formation of three-dimensional structures with participation of the fire-retarding constituents, and the serviceability of the fiberboards in an alternating climate is discussed. (R.E.)

NARAYANAMURTI, D. AND K. R. BIRJE. 1969. The influence of loading on the rigidity modulus and plastic flow in wood—Influence of impregnants. *Holzforsch. Holzverwert.* 21(6):136–140(E.g). The influence of various chemicals on the modulus of rigidity and plastic flow of eight different species of Indian woods was evaluated. The specimens were soaked for 15 days in six different chemicals and water, and the modulus of rigidity was then measured by vibrational methods. The effect varied with the wood species and the chemical. (D.M.)